

Identification of field dwarfs and giants in RAVE

S. Bilir,^{1*} S. Karaali², S. Ak¹, Ö. Önal¹, B. Coşkunoğlu¹, G. M. Seabroke³

¹*Istanbul University Science Faculty, Department of Astronomy and Space Sciences, 34119, University-Istanbul, Turkey*

²*Beykent University, Faculty of Science and Letters, Department of Mathematics and Computer, Beykent 34398, Istanbul, Turkey*

³*Mullard Space Science Laboratory, University College London, Hombury St Mary, Dorking, RH5 6NT, UK*

Accepted 2011 month day. Received year month day;

ABSTRACT

The second RAdial Velocity Experiment (RAVE) Data Release (DR2) derives $\log g$ values but we present a simpler and cleaner method of identifying dwarfs and giants using only magnitudes, which does not require spectroscopic analysis. We confirm the Bilir et al. (2006) procedure which estimates the number of dwarfs and giants via their positions in the $J - V$ two magnitude diagram by applying it to RAVE DR2. It is effective in estimating the number of dwarfs and giants at $J - H > 0.4$ compared to RAVE's $\log g$ values. For $J - H \leq 0.4$, where dwarfs and subgiants show a continuous transition in the J magnitude histogram, we used the Besançon Galaxy model predictions to statistically isolate giants. The percentages of giants for red stars and for the whole sample are 85% and 34%, respectively. If we add the subgiants, the percentage of evolved stars for the whole sample raises to 59%. For the first time in the literature, we analysed the effect of CHISQ on RAVE's $\log g$ values (CHISQ is the penalised χ^2 from RAVE's technique of finding an optimal match between the observed spectrum and synthetic spectra to derive stellar parameters). Neither the CHISQ values nor the signal-to-noise ratio bias RAVE $\log g$ values. Therefore the method of identifying dwarfs and giants via the two magnitude diagram has been verified against an unbiased dataset.

Key words: surveys–catalogues–techniques: photometric

* E-mail: sbilir@istanbul.edu.tr

1 INTRODUCTION

Large surveys such as the Two Micron All Sky Survey (2MASS, Skrutskie et al. 2006), Sloan Digital Sky Survey/Sloan Extension for Galactic Understanding and Exploration (SDSS/SEGUE, York et al. 2000; Yanny et al. 2009) and the RAdial Velocity Experiment (RAVE, Steinmetz et al. 2006) give the opportunity to a researcher to investigate different topics. However, one needs to select the appropriate data from these surveys and to classify them according to his/her aim. RAVE provides spectroscopic data observed from the southern hemisphere. Radial velocities are available in the first data release (DR1, Steinmetz et al. 2006) and spectroscopic analyses to provide information on values of stellar parameters (temperature, surface gravity and metallicity) are also included in the second data release (DR2, Zwitter et al. 2008) additional to the radial velocities. One can find the stellar parameters in the literature supplemented by stellar position, proper motion and photometric measurements from the Deep Near Infrared Survey of the Southern Sky (DENIS, Fouque et al. 2000), 2MASS (Skrutskie et al. 2006) and Tycho-2 (Høg et al. 2000) surveys.

Examples of scientific use of such a dataset are described in Steinmetz (2003). They include the identification and study of the current structure of the Galaxy and of remnants of its formation, recent accretion events, as well as discovery of individual peculiar objects and spectroscopic binary stars. For example, kinematic information derived from the RAVE dataset has been used to demonstrate the presence of a dark halo in the Galaxy (Smith et al. 2007). Veltz et al. (2008) identified kinematical discontinuities in the direction to the Galactic poles which separate a thin disc, thick disc and a hotter component. Seabroke et al. (2008) searched for infalling stellar streams onto the local Galactic disk and found that it is devoid of any vertically coherent streams containing hundreds of stars. Coşkunoğlu et al. (2011) estimated Local Standard of Rest (LSR) values from RAVE DR3. Klement et al. (2011) classified the dwarfs and giants in RAVE and used this classification in stellar stream detection.

Classification of stars in RAVE as dwarf and giant populations is also the topic of this paper. However, the procedure we use here is different. We use the positions of stars in the $J - V$ two magnitude diagram to estimate the number of dwarfs and giants of the sample considered. According to this procedure, stars which lie above the line fixed by Bilir et al. (2006) are dwarfs and those below the same line are giants. We show that this procedure provides accurate estimations compared to RAVE DR2 $\log g$ values. Also, it can be applied

without the following considerations of Klement et al. (2011) and hence provides simplicity: *i*) the gravity of a given luminosity class changes with colour, *ii*) reddening of stars causes to a less clear separation of dwarfs from other luminosity classes in $\log g$ distribution, *iii*) the dwarf-giant separation gets better with increasing colour, *iv*) the expected small fraction of dwarfs in combination with their higher $\log g$ uncertainties might hinder a clear separation and *v*) the $\log g$ distribution has been shown to vary with Galactic latitude.

Our work is the first one in the literature to analyse the effect of CHISQ in the RAVE data. CHISQ is the penalised χ^2 from RAVE’s technique of finding an optimal match between the observed spectrum and synthetic spectra to derive stellar parameters. It is conceivable that sample stars with large CHISQ and/or small signal-to-noise ratios (S/N) contaminate the dwarf and giant separation with unreliable $\log g$ values. We investigate whether CHISQ or S/N biases RAVE $\log g$ values and therefore biases the verification of our method of identifying dwarfs and giants via the two magnitude diagram.

The paper is organized as follows: the data and field dwarf-giant separation are given in Sections 2 and 3, respectively. Confirmation of field dwarf-giant separation and the effects of S/N and χ^2 on the separation of dwarfs and giants are presented in Sections 4 and 5 and finally a summary and discussion is devoted to Section 6.

2 DATA

The data were taken from the RAVE DR2 (Zwitter et al. 2008). Among 51 829 objects contained in RAVE DR2, only 49 327 objects are unique, the rest are repeated observations of single stars (Zwitter et al. 2008). We prepared our sample by applying the following constraints: *i*) $0 < \log g \leq 5$ and *ii*) $7.7 < V_T \leq 12.6$, where V_T is the visual apparent magnitude in Tycho-2 (Høg et al. 2000). Thus, the total number of our sample was reduced to 11 470 stars, from which we expect more reliable surface gravities and magnitudes. Along with $\log g$ values, *2MASS* (J , H and K_s) and Tycho-2 (B_T , V_T) apparent magnitudes are also available in RAVE DR2. As we need Johnson’s apparent V magnitude, we transformed the magnitudes B_T and V_T to Johnson’s V magnitude by the following equation in the Hipparcos catalogue (ESA 1997):

$$V = V_T - 0.09 \times (B_T - V_T) \tag{1}$$

The errors in Tycho magnitudes propagate 0.16 mag for V magnitude.

Zwitter et al. (2010) estimates the distances of K0 dwarfs to be between 50 and 250 pc, which encouraged us to neglect extinction for dwarfs. Although K0 giants are located at distances 0.7-3 kpc, their Galactic latitudes are absolutely larger than 20° . Hence, no dereddening was applied to the V and J apparent magnitudes used in the procedure which separates dwarfs and giants in our work.

To confirm our argument, we adopted the $(J - H) = 0.27$ and $(J - H) = 0.52$ (see Fig. 1) as the typical colours of FG dwarfs and K giants, respectively and transformed them to M_J magnitudes, i.e. 3.35 and 1.67 via the calibrations of Bilir et al. (2008) and the table of Covey et al. (2007). The combination of these absolute magnitudes with the apparent J magnitudes $5.5 \leq J \leq 12$ provides distance for a given star. We estimated $d \sin(b)$ distances to the Galactic plane for a set of directions defined by the Galactic latitudes $b = (30^\circ, 50^\circ, 75^\circ)$ and Galactic longitudes $l = (0^\circ, 90^\circ, 180^\circ, 270^\circ)$ and transformed the corresponding extinctions from Schlegel et al. (1998) maps to the distance in question by the following equation (Bahcall & Soneira 1980):

$$A_d(b) = A_\infty(b) \left[1 - \exp\left(\frac{-|d \sin(b)|}{H}\right) \right]. \quad (2)$$

Here, b and d are the Galactic latitude and distance of the star, respectively. H is the scaleheight for the interstellar dust which is adopted as 125 pc (Marshall et al. 2006) and $A_\infty(b)$ and $A_d(b)$ are the total absorptions for the model and for the distance to the star, respectively. $A_\infty(b)$ can be evaluated by means of Eq. (3):

$$A_\infty(b) = 3.1E_\infty(B - V). \quad (3)$$

$E_\infty(B - V)$ is the colour excess for the model taken from the NASA Extragalactic Database¹. Then, $E_d(B - V)$, i.e. the colour excess for the corresponding star at the distance d , can be evaluated by Eq. (4) adopted for distance d ,

$$E_d(B - V) = A_d(b) / 3.1. \quad (4)$$

The numerical ranges for $E_d(B - V)$ for dwarfs and giants, evaluated by this procedure for $|b| > 20^\circ$, are [0.001, 0.063], [0.003, 0.071], respectively. Hence, we can neglect the interstellar extinction in our work.

¹ <http://nedwww.ipac.caltech.edu/forms/calculator.html>

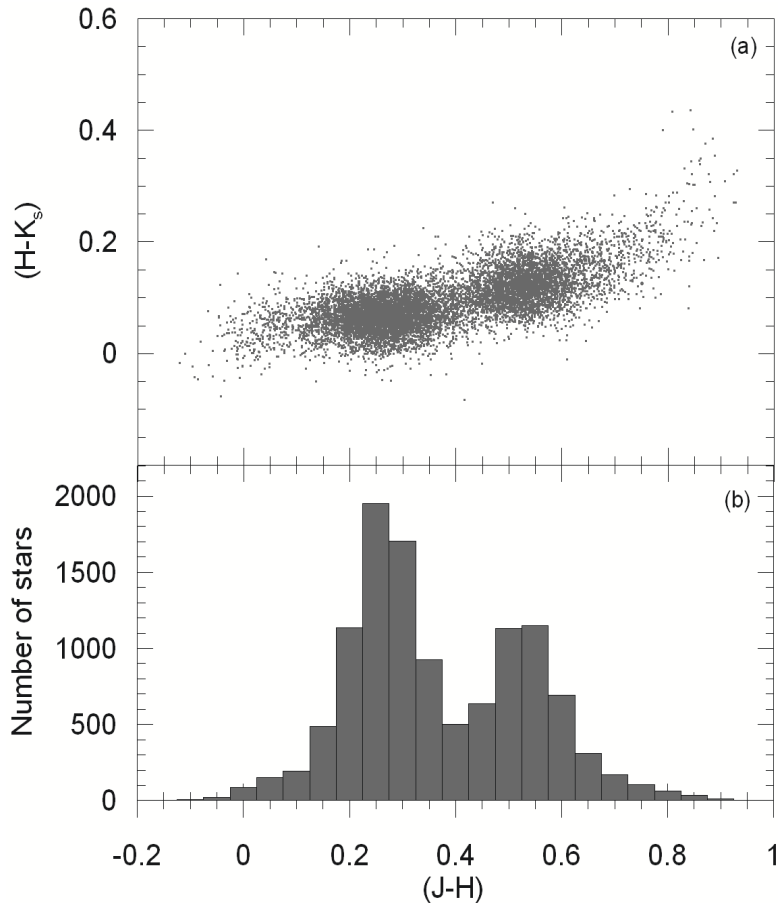


Figure 1. The star sample divided into two subsamples at $J - H = 0.4$ in the $(J - H) - (H - K_s)$ two-colour diagram (a). Distribution of stars according to their $(J - H)$ colours (b).

3 IDENTIFICATION OF DWARFS AND GIANTS VIA TWO BANDS

We adopted the procedure of Bilir et al. (2006) to identify the dwarfs and giants in our sample. Bilir et al. (2006) generated an empirical separation line to define dwarf and giant stars in the two selected star fields by their *2MASS* and *V* magnitudes. The separation lines were formulated through $V - J$, $J - H$ and $V - K_s$ magnitudes diagrams in these equations: $J = 0.957 \times V - 1.079$; $H = 0.931 \times V - 1.240$; $K_s = 0.927 \times V - 1.292$. According to this procedure, stars which lie above this line were classified as dwarfs, whereas those lie below this line were classified as giants. In this study, J versus V magnitude diagrams are used and stars with $J > 0.957 \times V - 1.079$ are expected to be dwarfs whereas those with $J \leq 0.957 \times V - 1.079$ are expected to be giants. The procedure was derived from spectroscopic data, hence its confidence level is high. We approach this problem as explained in the following.

First of all, we plotted the $(J - H)$ - $(H - K_s)$ two colour diagram of the sample stars. Fig. 1 reveals two subsamples separated by the colour $J - H = 0.4$ mag, keeping in mind that the

Table 1. Comparison of percentages of dwarfs and giants in our RAVE sample.

Subsample	Number of dwarfs		Number of giants	
	Total	%	Total	%
$\log g \leq 4, J - H \leq 0.4$	2520	98.78	31	1.22
$\log g \leq 4, J - H > 0.4$	484	11.95	3567	88.05
$\log g > 4, J - H \leq 0.4$	4357	98.84	51	1.16
$\log g > 4, J - H > 0.4$	211	45.87	249	54.13

dwarf-giant separation is colour dependent. Dwarfs are characterized by larger $\log g$ surface gravities relative to giants. Hence, we combined $\log g$ with $J - H$ colours to proceed in our study. We adopted $\log g = 4$ as a rough limit for separating dwarfs and giants (subgiants were not taken into account in the procedure of Bilir et al. (2006), hence we do not consider them in this section, but see the following sections). Thus we applied the procedure of Bilir et al. (2006) to four subsamples of stars, i.e. I: ($J - H \leq 0.4, \log g \leq 4$), II: ($J - H > 0.4, \log g \leq 4$), III: ($J - H \leq 0.4, \log g > 4$) and IV: ($J - H > 0.4, \log g > 4$), in order to separate dwarfs and giants in these subsamples (see Table 1). Fig. 2 shows that the majority of stars (3567) in the subsample II are giants, whereas only 484 stars which correspond to 12% of the total stars in this subsample are dwarfs. Stars in subsample III consist of dwarfs (4357); only 1% of the total stars in this subsample are giants and the number of dwarfs and giants are almost equal in subsample IV. In subsample I, the number of dwarfs is 2520, corresponding to 99% of the total number of stars in this subsample. This is an unexpected given that subsample I is defined to only include stars with $\log g \leq 4$ i.e. the $\log g$ values should be too low to be dwarfs.

Hence, we separated the subsample I into three extra subsamples, i.e. Ia: $\log g \leq 3$, Ib: $3 < \log g \leq 3.5$ and Ic: $3.5 < \log g \leq 4$ (Fig. 3), in order to treat the problem in detail. The J versus V magnitude diagram for subsample Ic classifies the majority of these stars as dwarfs: 2005 out of 2021 stars (99%), like subsample I. However, the number of dwarfs with $3 < \log g \leq 3.5$ in subsample Ib and even those with $\log g \leq 3$ in Ia are still much larger than the number of giants, i.e. they consist of more than 95% of the total number of stars. This is an unexpected result in the scheme of Bilir et al. (2006), which will be discussed in the following sections.

Additional to the error of 0.16 mag in V , mentioned in Section 2, another error originates from the transformation given in Bilir et al. (2006). The errors 0.16 and 0.024 mag in V and J , respectively, propagate 0.162 mag. This error causes a contamination of 12%

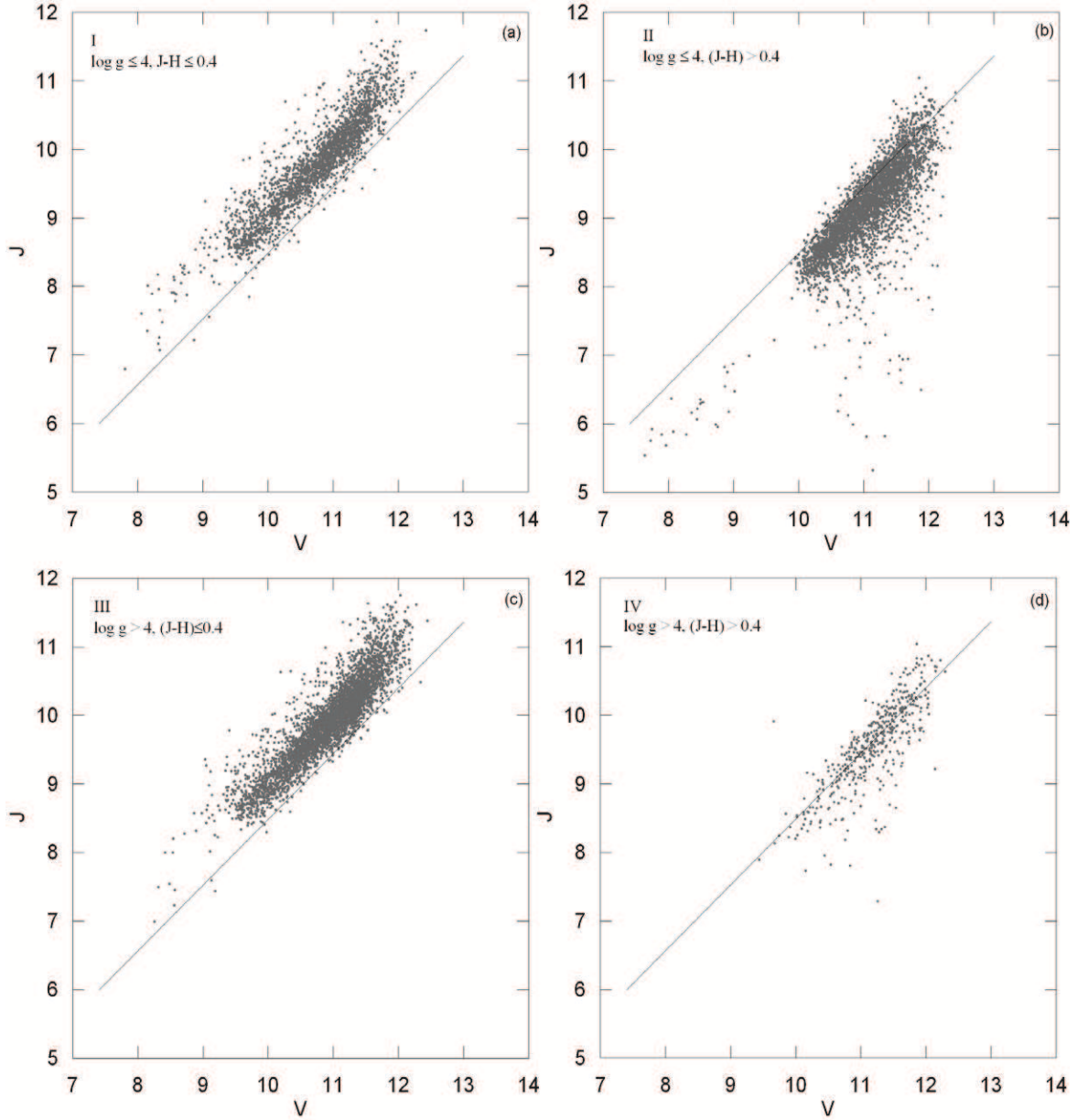


Figure 2. The J versus V magnitude diagrams of four subsamples: (a) I: $\log g \leq 4$ and $J - H \leq 0.4$. (b) II: $\log g \leq 4$ and $J - H > 0.4$. (c) III: $\log g > 4$ and $J - H \leq 0.4$. (d) IV: $\log g > 4$ and $J - H > 0.4$. The solid line represents the empirical dwarf-giant separation line of Bilir et al. (2006). The stars above the line are dwarfs, whereas those below the line are giants.

in the separation of dwarfs and giants via $J - V$ two magnitude diagram. However, this contamination is too small to be responsible for the results of subsamples I, Ia, Ib and Ic.

Table 2. Number of stars in six subsamples investigated in our work and those which appear in Ammons et al. (2006). The next two columns correspond to the number of stars with signal to noise ratio less than 13 and 33, respectively, and χ^2 range.

Subsample	Ammons et al. (2006)					Bilir et al. (2006)					Signal-to-Noise		
	Dwarf		Giant		Total	Dwarf		Giant		Total	S/N \leq 13	S/N \leq 33	χ^2 range
	N	(%)	N	(%)		N	(%)	N	(%)		N	N	
Ia	48	98	2	4	50	92	95	5	5	97	2	31	[240, 22502]
Ib	276	98	5	2	281	423	98	10	2	433	7	86	[074, 10579]
Ic	1335	99	12	1	1347	2005	99	16	1	2021	13	329	[075, 11826]
II	118	04	3237	96	3355	484	12	3567	88	4051	18	428	[024, 16633]
III	2938	98	46	2	2984	4357	99	51	1	4408	47	950	[046, 13029]
IV	80	35	146	65	226	211	46	249	54	460	10	90	[045, 09585]
Total	4795	100	3448	100	8243	7572	100	3898	100	11470	97	1914	

4 CONFIRMATION OF THE IDENTIFICATION OF DWARFS AND GIANTS VIA TWO BANDS

4.1 Confirmation with the data appeared in the literature

We confirm the identification of the dwarfs and giants in our work by comparing their positions with Ammons et al. (2006)’s FGK dwarfs in the $V - J$ two magnitude diagram. Ammons et al. (2006) used spline functions of broadband photometry and estimated fundamental astrophysical parameters, i.e. distance, effective temperature, and metallicity, for more than 100 000 dwarfs. The empirical broadband models are functions of Tycho-2 (B_T, V_T) and $2MASS$ (J, H, K_s) magnitudes and proper motions for FGK type stars.

We separated the stars of Ammons et al. (2006) into six subsamples defined by the $\log g$ surface gravities and $J - H$ colours used for the definition of subsamples Ia, Ib, Ic, II, III and IV (Table 2) and plotted them in Fig. 4. Afterwards, we compared them with the stars investigated in our work. We note that the stars of Ammons et al. (2006), which were taken from the Tycho-2 catalogue, are partly observed in the RAVE survey. The comparison of the two magnitude diagram positions of the stars common to both Ammons et al. (2006) and RAVE is limited. However, there are enough stars to obtain some results by this comparison (see Table 2). The identification of dwarfs and giants by Ammons et al. (2006) is based on atmospheric parameters. Hence, its accuracy is high.

There are 48 dwarfs and two giants with $\log g \leq 3$ and $J - H \leq 0.4$ in the catalogue of Ammons et al. (2006) whose positions fit with the dwarf and giant half planes in Fig. 4a. Contrary to the expectation due to small surface gravities, this is a strong confirmation that 92 stars out of 97 in Fig. 3a are dwarfs.

276 dwarfs and five giants of Ammons et al. (2006) with $3 < \log g \leq 3.5$ and $J - H \leq 0.4$

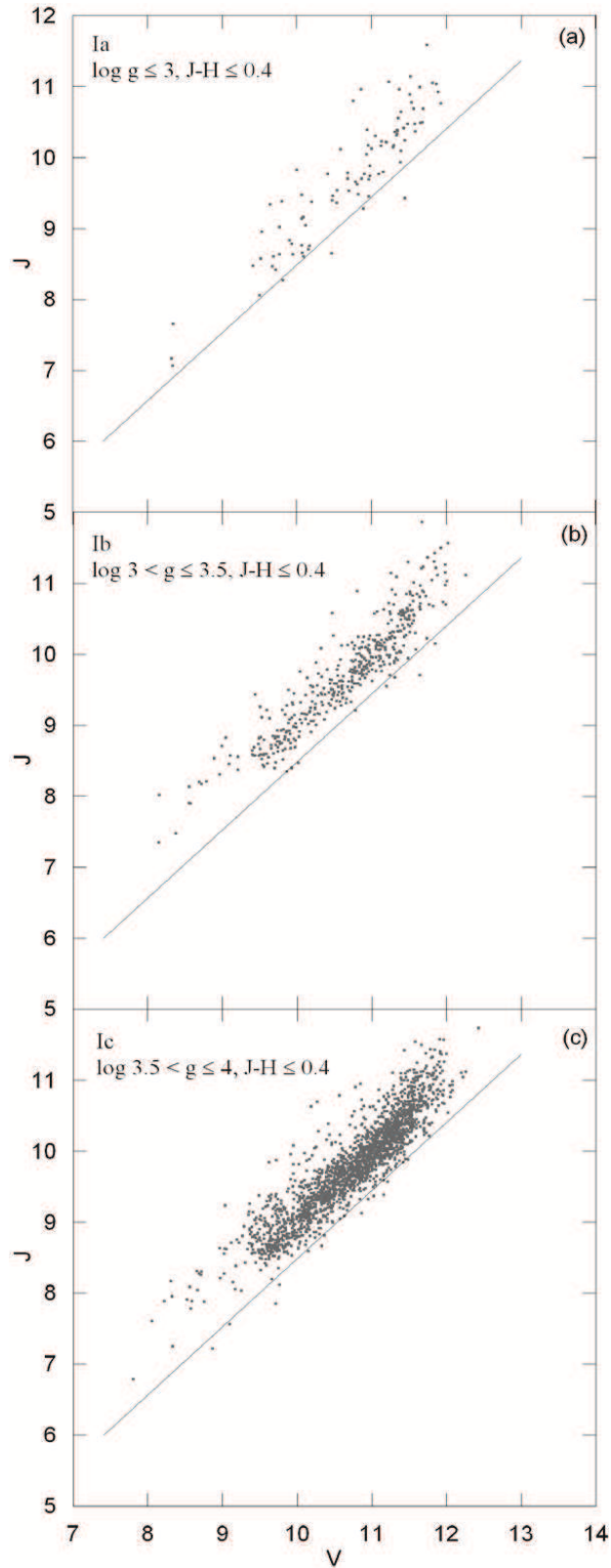


Figure 3. Stars in subsample I ($\log g \leq 4$ and $J - H \leq 0.4$) divided into three extra subsamples according to their $\log g$ values: (a) Ia: $\log g \leq 3$. (b) Ib: $3 < \log g \leq 3.5$. (c) Ic: $3.5 < \log g \leq 4$. The solid line represents the empirical dwarf giant separation line of Bilir et al. (2006). The stars above the line are dwarfs, whereas those below the line are giants.

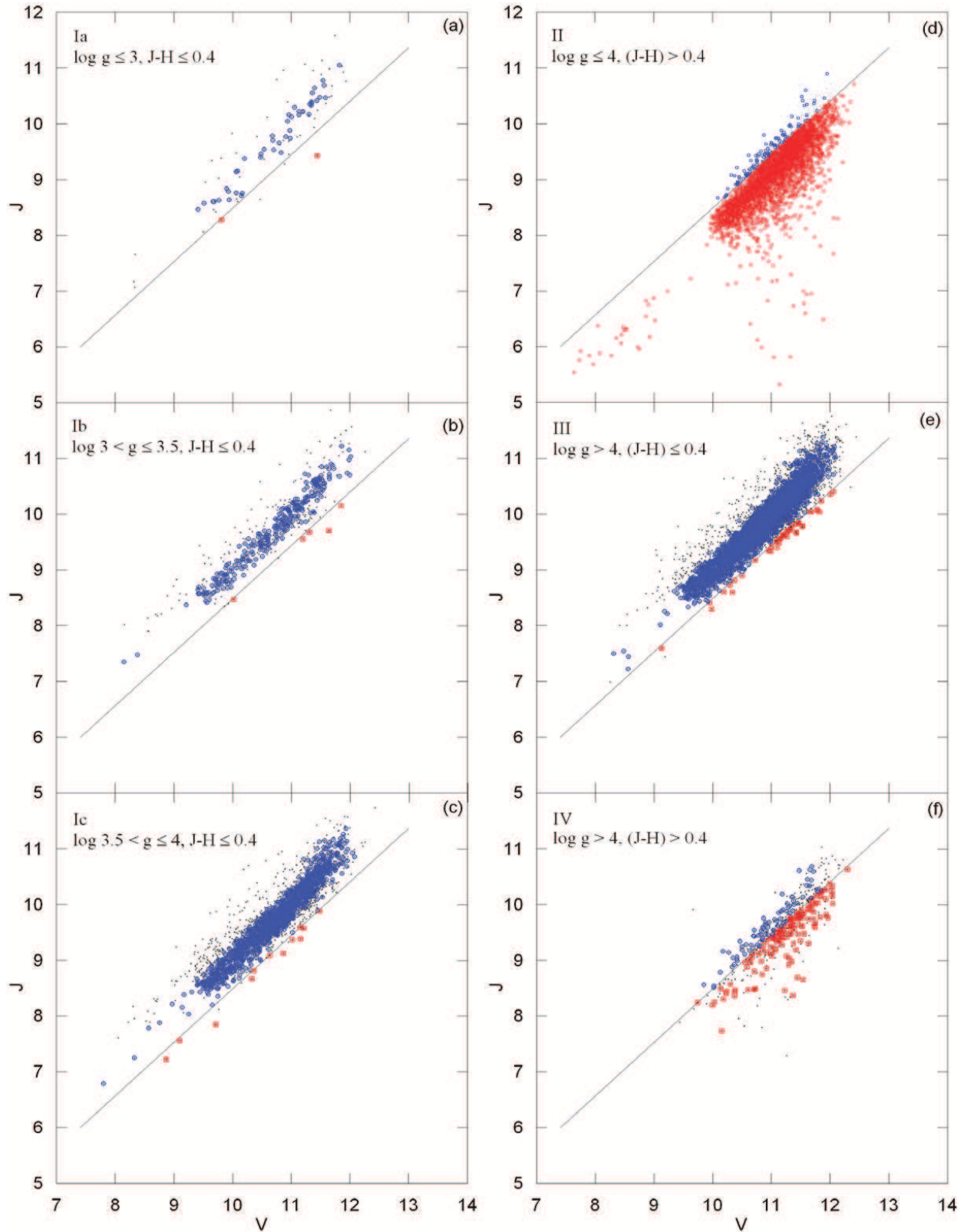


Figure 4. Stars in six subsamples, i.e. (a) Ia, (b) Ib, (c) Ic, (d) II, (e) III and (f) IV, plotted along with Ammons et al. (2006)'s stars. Filled circles denote RAVE dwarfs and giants, whereas open circles and squares denote dwarf and giant stars of Ammons et al. (2006), respectively. The solid line represents the empirical dwarf giant separation line of Bilir et al. (2006). The stars above the line are dwarfs, whereas those below the line are giants. The Roman numerals denote the subsamples explained earlier.

occupy the dwarf and giant half planes, respectively, in Fig. 4b, confirming that 423 stars with the same surface gravities and colours in our work which occupy the dwarf half plane are dwarfs. 10 stars (2% of the total stars) in Fig. 3b which occupy the giant half plane should be giants.

We noted in the preceding section that most of the stars with $3.5 < \log g \leq 4$ and $J - H \leq 0.4$ should be dwarfs. Actually, 2005 dwarfs, taken from Ammons et al. (2006), with the same surface gravities and colours confirm our suggestion (Fig. 4c). Additionally, 12 stars out of 16 (Fig. 3c) which were classified as giants in Ammons et al. (2006) occupy the giants' half plane, confirming the procedure which separates dwarfs and giants via two bands.

The data of Ammons et al. (2006) confirms also the results, obtained and noted in Section 3, for subsamples II ($\log g \leq 4$, $J - H > 0.4$), III ($\log g > 4$, $J - H \leq 0.4$) and IV ($\log g > 4$, $J - H > 0.4$) i.e. stars identified as dwarfs and giants in Ammons et al. (2006) occupy the dwarf and giant half planes in the panels Fig. 4d, 4e and 4f, respectively. Giants dominate in panel Fig 4d, whereas the majority of stars in panel Fig. 4e are dwarfs. As expected, panel Fig. 4f involves both populations, giants and dwarfs, in large numbers.

The values in the two columns before the last one denote to the number of stars with signal to noise ratio $(S/N) \leq 33$ and $(S/N) \leq 13$, corresponding to the mean $(S/N) - 1\sigma$ and $(S/N) - 2\sigma$, respectively, where $\sigma = 20$ is the standard deviation of S/N. These stars do not show any positional systematic difference relative to the ones with higher S/N, in the $J - V$ two magnitude diagram. Finally, the values in the last column are the CHISQ values (see Section 5 for details).

4.2 Confirmation with surface gravity–colour diagram

We plot all subsamples of stars, Ia, Ib, Ic, II, III and IV in the $\log g$ surface gravity and $J - H$ colour diagram and discuss their identifications (Fig. 5). Furthermore, isochrones are overlaid on the data in order to distinguish the dwarf region in the $J - H$ versus $\log g$ diagram. The isochrones are from the Padova database (Marigo et al. 2008), using the web interface². For our sample of stars, we adopted isochrones with metallicity $-2 \leq [M/H] \leq +0.2$ dex with 0.5 dex intervals for ages 1, 5 and 10 Gyrs. In total, 18 isochrones are plotted over the data in the $\log g$ versus $J - H$ diagram (Fig. 5).

² <http://stev.oapd.inaf.it/cgi-bin/cmd>

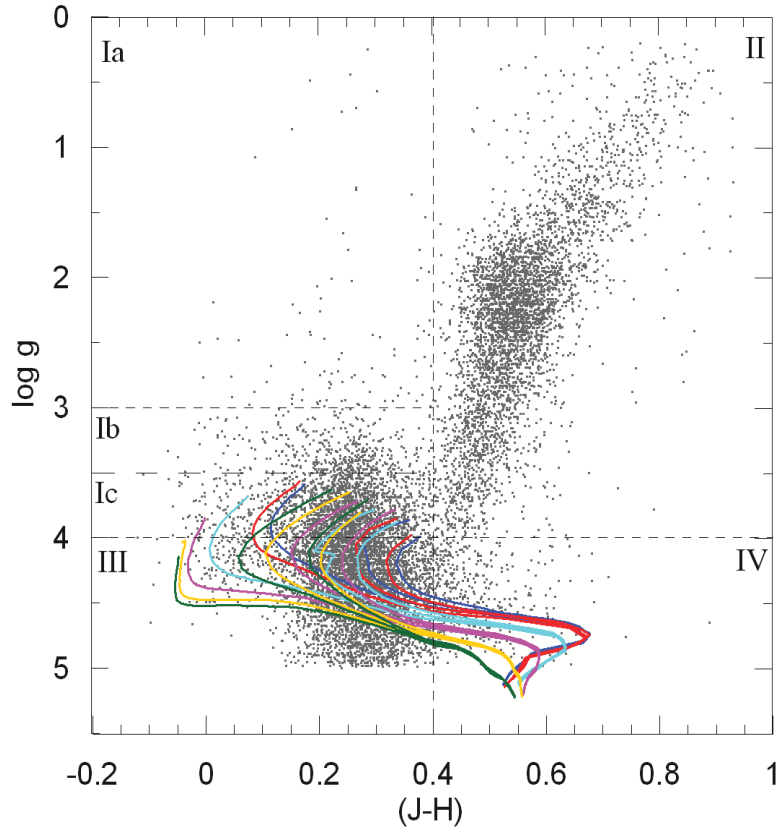


Figure 5. The $\log g$ versus $J-H$ diagram of the sample. Coloured lines denote the Padova isochrones with different metallicities ($-2 \leq [M/H] \leq 0.2$ dex) and ages (for 1, 5 and 10 Gyrs). The rectangles represent subsamples.

Most of the stars in subsample II ($\log g \leq 4$, $J-H > 0.4$) should be red giants. This is the case in Fig. 2b, i.e. 3567 giants and 484 dwarfs could be identified according to their positions in the J versus V magnitude diagram. Dwarfs correspond to only 12% of the total subsample.

Another confirmation can be done easily for stars in subsample III ($\log g > 4$, $J-H \leq 0.4$). The large surface gravities and their positions on the disk population isochrones of these stars indicate that they should be dwarfs. Actually, the number of dwarfs identified by their position in Fig. 2c consists of 99% of the total stars of this subsample.

Almost half of the stars in subsample IV ($\log g > 4$, $J-H > 0.4$) lie on the main sequence of the isochrones. Hence, these stars with large surface gravities should be dwarfs. The gap in the isochrones at $J-H > 0.4$ between the dwarf branch (shown in Fig. 5 panel IV) and the giant branch (giants are plotted in Fig. 5 panel II but the corresponding isochrone is not shown) suggests there should not be any stars with $J-H > 0.4$ and $4 < \log g < 4.5$. However, Fig. 5 shows data exist in this region. These are most likely to be due to measurement errors on $\log g$. RAVE DR2 $\log g$ errors are conservatively estimated to be 0.5 dex for an average $S/N \sim 40$. This is large enough that dwarfs with $\log g > 4.5$ can be

measured to have $\log g > 4$ and giants with $\log g < 4$ can be measured to have $\log g < 4.5$. This agrees with our argument that the number of dwarfs and giants in the subsample IV are almost equal (Fig. 2d).

Confirmation of dwarfs and giants identified by two bands, J and V , for subsamples Ia and Ib with the diagram surface gravity versus colour is not easy (Fig. 5). Although 95% of the total stars in subsample Ia ($\log g \leq 3$, $J - H \leq 0.4$) occupy the dwarf half plane, their surface gravities are rather small. Almost the same case holds for stars in subsample Ib ($3 < \log g \leq 3.5$, $J - H \leq 0.4$) where surface gravities have an upper limit of $\log g = 3.5$. Most of the stars in the subsample Ic ($J - H \leq 0.4$, $3.5 < \log g \leq 4$) lie on the subgiants segments of the isochrones, indicating that they are subgiants rather than dwarfs. Hence, we should add a procedure to the one of Bilir et al. (2006) for separation of subgiants from dwarfs and giants.

4.3 Number of Stars for Different Populations Estimated via Galaxy Model

We use the Besançon Galaxy model (Robin et al. 2003) to estimate the number of stars for different populations, i.e. dwarf, subgiant and giant, in our sample and compared them with the ones obtained by using the procedure of Bilir et al. (2006). The Besançon Galaxy model of stellar population synthesis is a simulation tool used to test Galaxy evolution scenarios by comparing stellar distributions predicted by these scenarios with observations, such as photometric star counts and kinematics. The model assumes that stars are created from gas following a star formation history and an initial mass function; stellar evolution follows evolutionary tracks (Schultheis et al. 2006).

We applied the model to stars with $0 < J - H \leq 0.4$ (sample 1) and $0.4 < J - H \leq 1$ (sample 2) separately. The restrictions used for the model are as follows: $d \leq 2$ kpc, size: one square degree, $7.7 < V \leq 12.6$, zero absorption, $0 < B - V \leq 0.8$ (for sample 1) and $0.8 < B - V \leq 1.63$ (for sample 2). The model has been applied to 12 directions of the Galaxy and the number of stars for each population has been estimated for each direction. The sets for Galactic latitude and longitude combined for the mentioned directions are: $|b| = (30^\circ, 50^\circ, 70^\circ)$ and $l = (0^\circ, 90^\circ, 180^\circ, 270^\circ)$. The results are given in Table 3. The number of stars for a particular population varies for different Galactic directions, as expected. Hence, we adopted the mean values for each population for sample 1 and sample 2.

As already seen in Fig. 5, there is an absence of subgiants in the sample of stars with

$0.4 < J - H \leq 1$ in Table 3, which gives us the chance to compare the number of giants and dwarfs claimed in Table 2 with the ones estimated via the Besançon Galaxy model. The number of giants in subsample II and subsample IV is 3816 which corresponds to 85% of the total number of stars with $0.4 < J - H \leq 1$. This is rather close to the corresponding model value, 82% (see Table 3), and of course the same holds for dwarfs, i.e. 15% observed and 18% in the model.

The Besançon Galaxy model predicts that 33% of the stars with $0 < J - H \leq 0.4$ will be subgiants and 2% will be giants. The number of giants for this colour claimed in Table 2 is 1%, in close agreement with the model. However, the procedure which separates dwarfs and giants via two bands has not been scaled for subgiant separation. Hence, we should find another procedure to carry out this work.

We plotted the histogram for J magnitudes for stars with $0 < J - H \leq 0.4$ and fitted it to a Gaussian curve (Fig. 6). The unique modality of the distribution shows that there is a continuous transition between dwarfs and subgiants when one goes from bright J magnitudes to the faint ones. A similar claim can be found in Klement et al. (2011) for $\log g$ of early type stars. However, we can find the number of subgiants in our work statistically, by adopting the model percentages given in the preceding paragraphs. 65% of the stars in a Gaussian distribution corresponds to 0.94 standard deviation of that distribution. Hence, stars with $0 < J - H \leq 0.4$ and, $\bar{J} < -0.94 \times s$ and $\bar{J} > +0.94 \times s$ will be considered as evolved (subgiants and giants) stars. Here, \bar{J} and s correspond to the mean and standard deviation, respectively. Thus, the total number of evolved stars and dwarfs in question are 2900 and 4060, respectively.

5 EFFECT OF S/N RATIO AND CHISQ VALUES ON IDENTIFICATION OF DWARFS AND GIANTS

5.1 The effect of S/N

Although the identification of dwarfs and giants via two bands have been confirmed in Section 4, one can argue that the positions of some stars in our work may be erroneously determined. Such an argument should be discussed for at least some subsamples of stars, such as subsample I ($\log g \leq 4$, $J - H \leq 0.4$). In subsample I, the majority of the involved stars are identified as dwarfs, though their surface gravities are small. If such a contamination exists it may originate from the small S/N ratios. For example as S/N decreases, the wings

Table 3. Percentages of dwarfs, subgiants and giants for our two $J - H$ colour intervals, for different Galactic directions estimated via the Besançon Galaxy model. The symbols l and b are Galactic longitude and latitude respectively.

Colour range →			$0 < J - H \leq 0.4$			$0.4 < J - H \leq 1$		
Galactic latitude ($^\circ$)	l ($^\circ$)	b ($^\circ$)	Giant (%)	Subgiant (%)	Dwarf (%)	Giant (%)	Subgiant (%)	Dwarf (%)
$20 < b < 40$	0	30	5.88	43.14	50.98	90.91	0.00	9.09
	90	30	5.26	45.61	49.12	88.24	0.00	11.76
	180	30	2.22	42.22	55.56	84.62	0.00	15.38
	270	30	6.35	39.68	53.97	92.00	0.00	8.00
$40 < b < 60$	0	50	2.86	31.43	65.71	80.00	0.00	20.00
	90	50	0.00	33.33	66.67	93.33	0.00	6.67
	180	50	0.00	53.57	46.43	100.00	0.00	0.00
	270	50	0.00	19.35	80.65	75.00	0.00	25.00
$60 < b < 90$	0	75	0.00	20.00	80.00	66.67	0.00	33.33
	90	75	0.00	8.33	91.67	60.00	0.00	40.00
	180	75	3.57	25.00	71.43	83.33	0.00	16.67
	270	75	0.00	33.33	66.67	66.67	0.00	33.33
Average (%)			2.18	32.92	64.91	81.73	0.00	18.27
This paper (%)			1.18	98.82*		84.59	15.41*	

* This symbol shows the percentage of the total number of subgiant and dwarf stars.

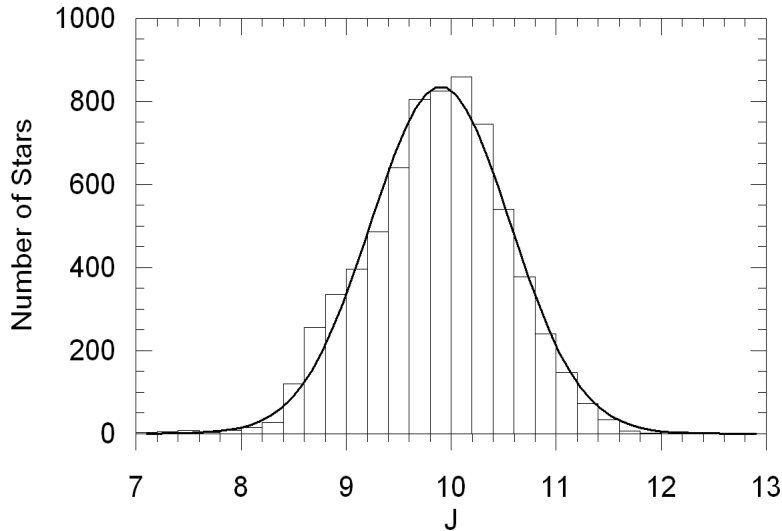


Figure 6. Histogram for J magnitudes for stars with $0 < J - H \leq 0.4$ fitted to a Gaussian curve. Single mode indicates to the continuous transition between dwarfs and subgiants (see the text).

of the spectral lines become more affected by noise, making them appear narrower, which could mimic a lower $\log g$.

The mean and the median of S/N ratios for all stars in our sample (11470 stars) are close to each other which indicates that S/N ratios form a Gaussian distribution. Their mean and standard deviation are 53 and 20, respectively. We adopted the 1914 stars with S/N ratios less than 33 (53-20) as candidates of contaminating our diagrams, and marked them with blue colours on the J versus V magnitude diagrams (Fig. 7) to treat the effect of S/N ratios on the identification of dwarfs and giants. Stars with $S/N > 33$ ratios are plotted on the same diagrams with their original symbols. One can not reveal any systematic scattering between

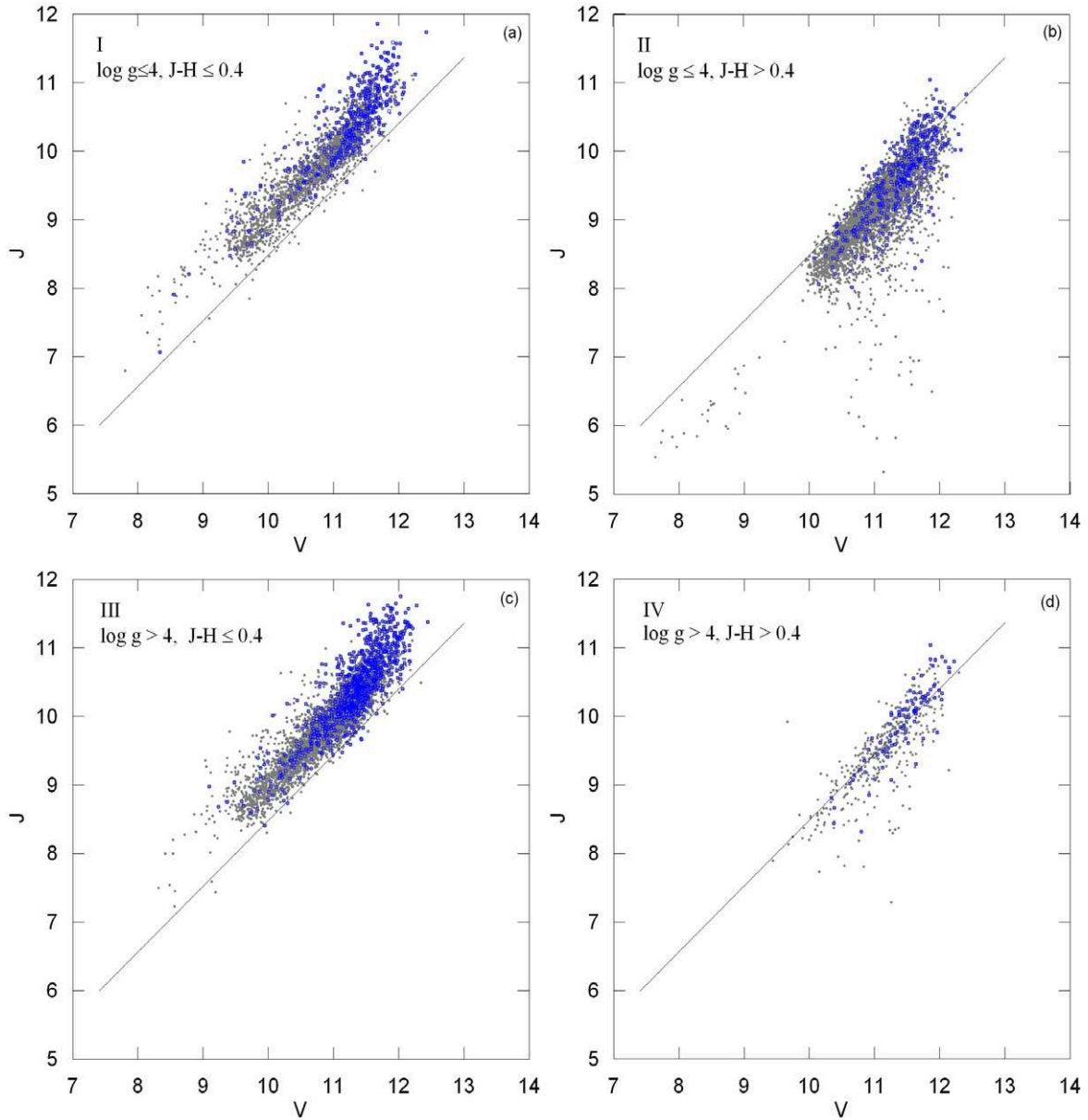


Figure 7. Investigating the effect of S/N ratios on the identification of dwarfs and giants. Stars with $S/N \leq 33$ (open blue circles) do not show any systematic distribution relative to stars which are confirmed as being giants/dwarfs (filled black circles).

two sets of S/N ratios, for subsamples I, II, III, and IV defined in the previous sections. For example, the S/N ratios for dwarfs with small $\log g$ surface gravities may be larger than 33 as well as smaller than this numerical value. The same result has been obtained for mean (S/N)- 2σ standard deviations, i.e. $S/N \leq 13$. Our conclusion is that small S/N ratios do not affect the identification of dwarfs and giants via two bands. The percentages of the stars with $S/N \leq 33$ are given in Table 4.

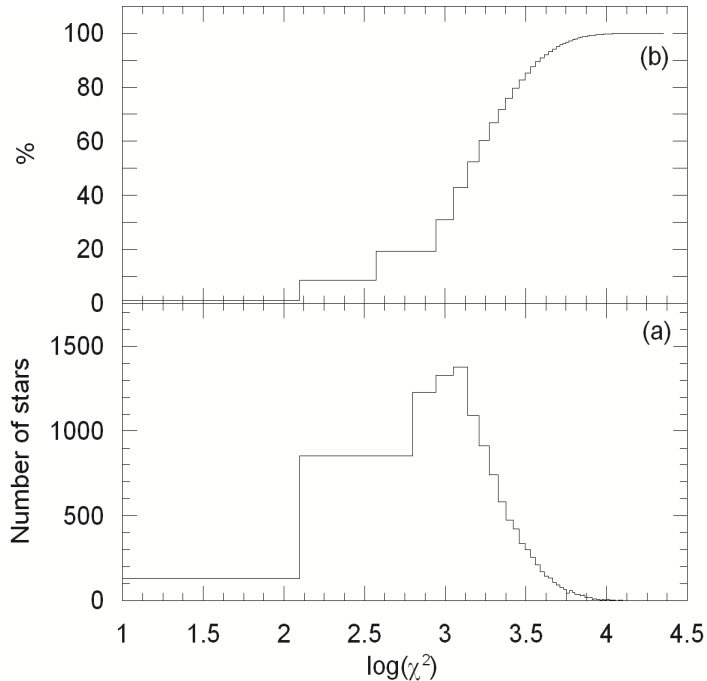


Figure 8. CHISQ histogram for stars in our sample (a). Stars with CHISQ values larger than 2290 consist 20% of the sample (b).

5.2 The effect of CHISQ

We checked whether the CHISQ values in RAVE DR2 bias the identification of dwarfs and giants. CHISQ is the penalised chi-squared from the technique finding an optimal match between the observed spectrum and the one constructed from a library of precomputed synthetic spectra to derive stellar parameters, including $\log g$. The spectral type of RAVE stars is generally not known and the input catalogue does not use any colour criterion. So, RAVE stars are expected to include all evolutionary stages and a wide range of masses in the HR diagram. However, the template library only covers normal stars. So, peculiar objects cannot be classified correctly. Sometimes a peculiar nature of the spectrum can be inferred from a poor match of the templates, despite a high S/N of the observed spectrum. This poor match of a spectrum to a template is quantified by CHISQ.

We used the CHISQ values of stars in our sample to treat this problem. These values lie between 24 and 22 503. We plotted their histogram in Fig. 8, and colour-coded stars whose CHISQs are larger than 2290 (20% of the whole sample) in the J versus V two magnitude diagram (Fig. 9). The distribution of CHISQ is not plotted or discussed in Zwitter et al. (2008). This is the first analysis of RAVE DR2’s CHISQ values to appear in the literature. As in Fig. 7, one can not reveal any systematic scattering between stars with CHISQ values larger and smaller than 2290 (20%). Hence, our conclusion is that the CHISQ values in RAVE

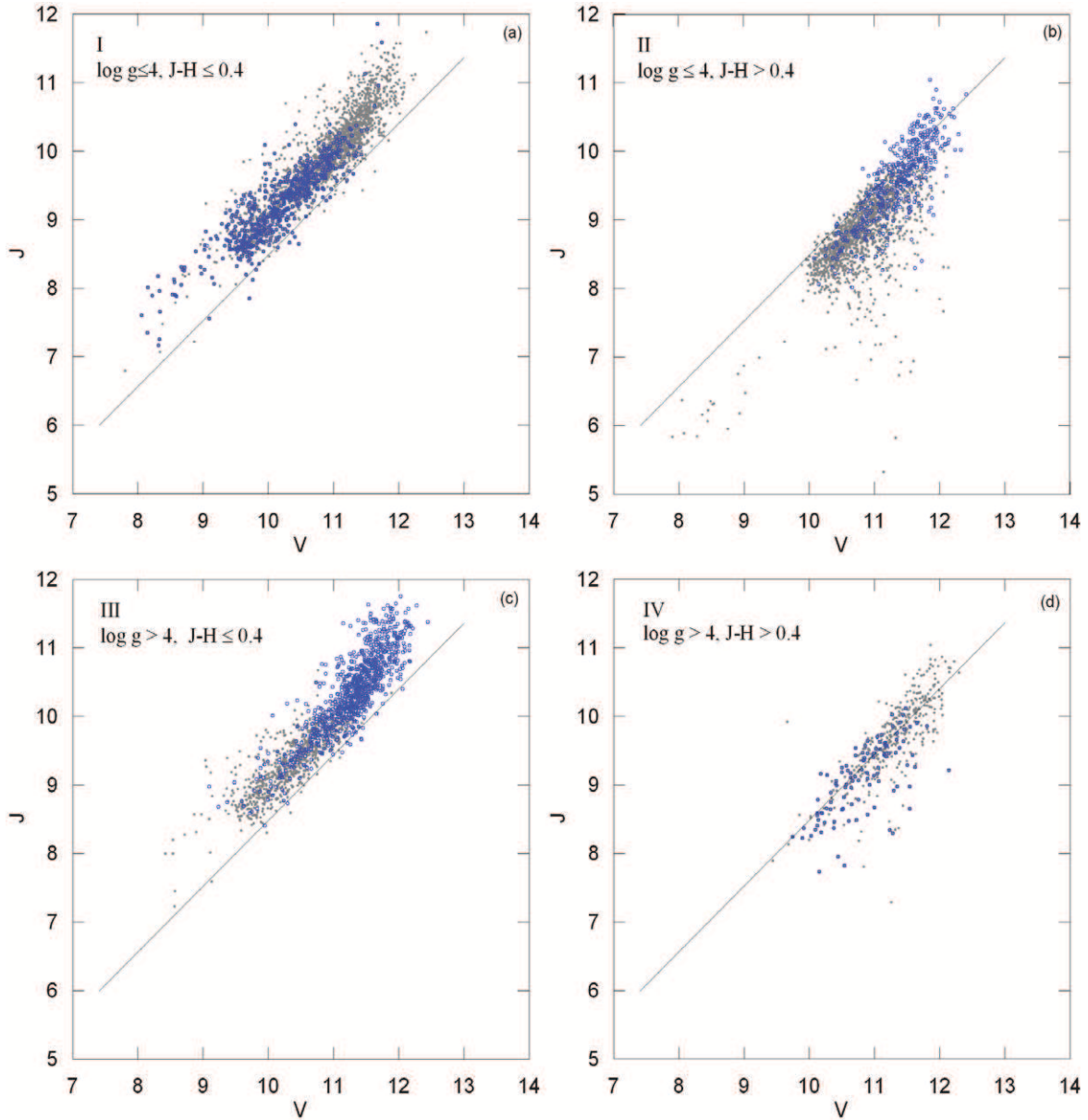


Figure 9. Investigating the effect of CHISQ on the identification of dwarfs and giants. Stars with CHISQ between 2290 and 22503 (20% of the sample, blue open circles) do not show any systematic distribution relative to stars with CHISQ less than 2290 (filled black circles).

DR2 do not bias the identification of dwarfs and giants via two bands. CHISQ distribution for the sample stars is given in Table 5.

6 SUMMARY AND DISCUSSION

We estimated the number of stars for different populations in the RAVE DR2 by means of their positions in the J versus V two magnitude diagram (Bilir et al. 2006) and the Besançon Galaxy model (Robin et al. 2003). The procedure of Bilir et al. (2006) is scaled for separation of dwarfs and giants (but not for subgiants). One can predict the number of

subgiants, additional to dwarfs and giants, via the Besançon Galaxy model. Different results were obtained for two samples of stars, i.e. for blue and red ones, separated by $J - H = 0.4$.

a) Sample of stars with $J - H > 0.4$: Dwarfs and giants in this sample have been separated in a very simple manner, i.e. by their positions in the $J-V$ two magnitude diagram. No additional constraints are needed for this separation. The percentages of dwarfs (15%) and giants (85%) are confirmed by the percentages of stars predicted by the Besançon Galaxy model, i.e. 18% dwarfs, 82% giants and no subgiants. A second confirmation was done using the work of Ammons et al. (2006). The positions of dwarf and giant in Ammons et al. (2006) occupy the dwarf and giant half planes in our work. Finally, the positions of the stars with $J - H > 0.4$ in the $\log g$ versus $J - H$ diagram indicate a large number of giants. Actually, most of these red stars have surface gravities less than the upper limit attributed to giants, i.e. $\log g = 3.8$ (Zwitter et al. 2010).

b) Sample of stars with $J - H \leq 0.4$: The separation of stars with $J - H \leq 0.4$ by means of their positions in the J versus V two magnitude diagram is not as easy as for stars with $J - H > 0.4$, because there is a considerable number of subgiants among these stars which were not scaled in Bilir et al. (2006). The procedure of Bilir et al. (2006) reveals 82 giants and 6877 dwarfs corresponding to 1% and 99% of the total number of stars, respectively. However, the percentage number of giants, dwarfs and subgiants predicted by the Besançon model (Robin et al. 2003) are 2%, 65% and 33%, respectively. Hence, we plotted the histogram for J magnitude, for stars with $J - H \leq 0.4$ to investigate this problem. The unique modality of the distribution indicates that there is a continuous transition between dwarfs and subgiants. Hence, we applied the Besançon Galaxy model to this sample for estimation of the number stars for different populations. Thus, the number of dwarfs reduced to 58%, and the remaining 42% of the total sample turned out to be evolved stars (giants and subgiants).

It should be noted that dwarfs and giants with $J - H \leq 0.4$ in Ammons et al. (2006) confirm the dwarf and giant half planes, respectively, defined by J and V magnitudes. The identification of dwarfs and giants by Ammons et al. (2006) is based on atmospheric parameters. Hence, its accuracy is high.

c) Error in $\log g$: 18% of the total stars with $3.5 < \log g < 4$ in Fig. 5 occupy the subgiant segments of the isochrones. Hence, they should be subgiants. However, the percentages of subgiants predicted by the Besançon model is 25%. The difference between percentages

Table 4. Comparison of percentages of dwarfs and giants with different ranges of S/N.

Subsample	Number of dwarfs					Number of giants				
	Total	S/N \leq 33	%	S/N $>$ 33	%	Total	S/N \leq 33	%	S/N $>$ 33	%
$\log g \leq 4, J - H \leq 0.4$	2520	444	18	2076	82	31	2	7	29	93
$\log g \leq 4, J - H > 0.4$	484	112	23	372	77	3567	316	9	3251	91
$\log g > 4, J - H \leq 0.4$	4357	939	22	3418	78	51	11	22	40	78
$\log g > 4, J - H > 0.4$	211	51	24	160	76	249	39	16	210	84

can be explained by the estimated error on RAVE DR2 surface gravities being as large as 0.5 dex.

d) Effect of S/N and CHISQ values: We showed in this work that neither the small signal to noise ratio (S/N) nor the CHISQ values bias RAVE $\log g$ values. Therefore the method of identifying dwarfs and giants via the two magnitude diagram has been verified against an unbiased dataset.

e) Comparison between the results in our work and the ones apparent in the literature: The first estimate of the percentage of different stellar populations in RAVE was published in Seabroke et al. (2008). They used a reduced proper motion diagram to kinematically separate red ($J - K > 0.5$) giants from red ($J - K > 0.5$) dwarfs. Statistically, they found that 44% of their RAVE sample consisted of red ($J - K > 0.5$) giants and red ($J - K > 0.5$) subgiants. Although Seabroke et al. (2008) do not explicitly state their 44% sample includes subgiants, their fig. 13 shows the subgiant branch extends to redder colours than $J - K = 0.5$. Seabroke et al. (2008) do not distinguish between blue ($J - K < 0.5$) subgiants and blue ($J - K < 0.5$) dwarfs. Therefore Seabroke et al. (2008) do not provide an estimate for the percentage of evolved (subgiant and giant) stars in RAVE. Given their 44% sample excludes blue ($J - K < 0.5$) subgiants, 44% represents a lower limit on the percentage of evolved stars in RAVE, which is consistent with the value of 59% that we find in our work. It should also be noted that the Seabroke et al. (2008) RAVE sample consists of many more stars than DR2 ($\sim 200\,000$ stars compared to $\sim 50\,000$) so the density of sampling in different directions on the sky will be different between the two samples and so they are not suitable for detailed direct comparison. Klement et al. (2011) found 43% of RAVE DR2 are dwarfs (see completeness column in their table 3). The remaining 57% are subgiants, giants and supergiants, which agrees closely with our value.

As conclusion, stars with $J - H > 0.4$ can be separated into dwarf and giant populations in a very simple manner, i.e. by their positions in the $J - H$ two magnitude diagram. One does not need any other constraints for such a separation. Our argument has been confirmed

Table 5. Comparison of percentages of dwarfs and giants with different ranges of CHISQ (χ^2).

Subsample	Number of dwarfs					Number of giants				
	Total	$\chi^2 \leq 2290$	%	$\chi^2 > 2290$	%	Total	$\chi^2 \leq 2290$	%	$\chi^2 > 2290$	%
$\log g \leq 4, J - H \leq 0.4$	2520	1875	74	645	26	31	16	52	15	48
$\log g \leq 4, J - H > 0.4$	484	414	86	70	14	3567	2083	58	1484	42
$\log g > 4, J - H \leq 0.4$	4357	3541	81	815	19	51	40	78	11	22
$\log g > 4, J - H > 0.4$	211	177	84	34	16	249	178	71	71	39

by the work of Ammons et al. (2006) and the Besançon Galaxy model (Robin et al. 2003). However, the existence of a considerable number of subgiants complicates the separation of stars with $J - H \leq 0.4$ into different population types. The difference between the percentage of subgiants obtained via the $\log g$ versus $J - H$ diagram (18%) and the one estimated by using the Besançon Galaxy model (25%) supports the values in $\log g$ of RAVE dataset. The percentage of evolved (subgiant and giant) stars found in this work is consistent with Seabroke et al. (2008) and in close agreement with Klement et al. (2011). For the first time in the literature, we analysed the effect of the CHISQ in the RAVE data. Neither the CHISQ values nor the signal-to-noise ratio bias RAVE $\log g$ values. Therefore the method of identifying dwarfs and giants via the two magnitude diagram has been verified against an unbiased dataset.

7 ACKNOWLEDGEMENTS

We would like to thank the referee Dr. Antonio Cabrera-Lavers for his useful comments that improved the readability of this paper.

Funding for RAVE has been provided by: the Australian Astronomical Observatory, the Astrophysical Institute Potsdam, the Australian National University, the Australian Research Council, the French National Research Agency, the German Research Foundation, the Instituto Nazionale di Astrofisica at Padova, The Johns Hopkins University, the W.M. Keck Foundation, the Macquarie University, the Netherlands Research School for Astronomy, the Natural Sciences and Engineering Research Council of Canada, the Slovenian Research Agency, the Swiss National Science Foundation, the Science & Technology Facilities Council of the UK, Opticon, Strasbourg Observatory, and the Universities of Groningen, Heidelberg, and Sydney.

Salih Karaali is grateful to the Beykent University for financial support. This publication makes use of data products from the Two Micron All Sky Survey, which is a joint project of

the University of Massachusetts and the Infrared Processing and Analysis Center/California Institute of Technology, funded by the National Aeronautics and Space Administration and the National Science Foundation.

This research has made use of the SIMBAD database, operated at CDS, Strasbourg, France and NASA's Astrophysics Data System.

REFERENCES

- Ammons S. M., Robinson S. E., Strader J., Laughlin G., Fischer D., Wolf A., 2006, *ApJ*, 638, 1004
- Bahcall J. N., Soneira R. M., 1980, *ApJS*, 44, 73
- Bilir S., Karaali S., Güver T., Karataş Y., Ak S., 2006, *AN*, 327, 72
- Bilir S., Karaali S., Ak S., Yaz E., Cabrera-Lavers A., Coşkunoğlu K. B., 2008, *MNRAS*, 390, 1569
- Coşkunoğlu B., et al., 2011, *MNRAS*, 412, 1237
- Covey K. R., et al., 2007, *AJ*, 134, 2398
- ESA, 1997, *Hipparcos and Tycho Catalogues*, ESA SP-1200, 1, 57
- Fouque P., et al., 2000, *A&AS*, 141, 313
- Høg E. E., Fabricius C., Makarov V. V., Urban S., Corbin T., Wycoff G., Bastian U., Schwekendiek P., Wicenec A., 2000, *A&A*, 355, L27
- Klement R. J., Bailer-Jones C. A. L., Fuchs B., Rix H.-W., Smith K. W., 2011, *ApJ*, 726, 103
- Marigo P., Girardi L., Bresson A., Groenewegen M. A. T., Silva L., Granato G. L., 2008, *A&A*, 482, 883
- Marshall D. J., Robin A. C., Reylé C., Schultheis M., Picaud S., 2006, *A&A*, 453, 635
- Robin A. C., Reylé C., Derrière S., Picaud S., 2003, *A&A*, 409, 523
- Schlegel D. J., Finkbeiner D. P., Davis M., 1998, *ApJ*, 500, 525
- Schultheis M., Robin A., C., Reylé C., McCracken H. J., Bertin E., Mellier Y., Le Fèvre O., 2006, *A&A*, 447, 185
- Seabroke G. M., et al., 2008, *MNRAS*, 384, 11
- Smith M., et al., 2007, *MNRAS*, 379, 755
- Skrutskie M. F., et al., 2006, *AJ*, 131, 1163
- Steinmetz M., 2003, *ASP Conf. Ser.*, 298, 381

Steinmetz M., et al., 2006, AJ, 132, 1645

Veltz L., et al., 2008, A&A, 480, 753

Yanny B., et al., 2009, AJ, 137, 4377

York D. G., et al., 2000, AJ, 120, 1579

Zwitter T., et al., 2008, AJ, 136, 421

Zwitter T., et al., 2010, A&A, 522A, 54